

ARTICLE

Received 9 Jul 2015 | Accepted 22 Oct 2015 | Published 1 Dec 2015

DOI: 10.1038/ncomms9990

OPEN

High pressure effects revisited for the cuprate superconductor family with highest critical temperature

Ayako Yamamoto¹, Nao Takeshita², Chieko Terakura¹ & Yoshinori Tokura^{1,3}

How to enhance the superconducting critical temperature (T_c) has been a primary issue since the discovery of superconductivity. The highest T_c reported so far is 166 K in $\text{HgBa}_2\text{Ca}_2\text{Cu}_3\text{O}_{8+\delta}$ (Hg1223) at high pressure of 23 GPa, as determined with the reduction onset, but not zero, of resistivity. To clarify the possible condition of the real maximum T_c , it is worth revisiting the effects of pressure on T_c in the highest T_c family. Here we report a systematic study of the pressure dependence of T_c in $\text{HgBa}_2\text{CaCu}_2\text{O}_{6+\delta}$ (Hg1212) and Hg1223 with the doping level from underdoped to overdoped. The T_c with zero resistivity is probed with a cubic-anvil-type apparatus that can produce hydrostatic pressures. Variation, not only increase but also decrease, of T_c in Hg1212 and Hg1223 with pressure strongly depends on the initial doping levels. In particular, we confirm a maximum T_c of 153 K at 22 GPa in slightly underdoped Hg1223.

¹Strong Correlation Physics Division, RIKEN Center for Emergent Matter Science (CEMS), Wako 351-0198, Japan. ²Electronics and Photonics Research Institute, National Institute of Advanced Industrial Science and Technology (AIST), Tsukuba 305-8568, Japan. ³Department of Applied Physics, The University of Tokyo, Tokyo 113-8656, Japan. Correspondence and requests for materials should be addressed to A.Y. (email: ayako-yamamoto@riken.jp).

Knowledge of the effects of pressure on superconducting critical temperature (T_c) is of paramount importance for understanding the mechanism of superconductivity, as exemplified by the latest report on the pressure-induced above-200 K superconductivity¹. In the conventional superconductors such as MgB₂, T_c decreases with increasing pressure reflecting the decrease of density-of-states at the Fermi level², whereas in some of the unconventional superconductors such as FeSe, T_c increases with increasing pressure³ at least within a certain range of pressure. In the most of high- T_c superconductors (HTSCs) with CuO₂ layers, T_c increases with pressure in a manner strongly depending on the composition and doping level⁴.

Mercury-based HTSCs denoted as the general formula HgBa₂Ca_{n-1}Cu_nO_{2n+2+δ} ($n=1, 2, 3, 4, \dots$) show very high values of T_c already at ambient pressure (AP): 95, 127, 134, and 130 K for $n=1, 2, 3$, and 4, respectively⁵⁻⁷. Studies of pressure effects on T_c were started just after the discovery of this homologous series, and the maximum values of T_c for HgBa₂CaCu₂O_{6+δ} (Hg1212) and HgBa₂Ca₂Cu₃O_{8+δ} (Hg1223) were reported to be 154 K (ref. 8) and 166 K (ref. 9) at ~25 GPa, respectively. Gao *et al.*⁸ argued that a universal upward shift in T_c was a common feature for all Hg 12($n-1$)n. Although these values of T_c are commonly accepted, we believe they should be reinvestigated to better understand the effects of high pressures in the light of advances in materials synthesis and high pressure technique; these values of T_c were determined from the so-called onset temperature, at which resistivity begins to deviate at a steeper rate from those at higher temperatures with decrease of temperature, whereas the observation of zero resistivity, which literally defines superconductivity, was not attained. Furthermore, in previous studies the pressure above 10 GPa was generated with a diamond-anvil cell^{8,9}, which does not necessarily ensure the generation of pressures of excellent hydrostatic nature. For a precise study on effects of pressure on zero resistance T_c , high-quality hydrostatic pressures are required.

To address these issues, we have reinvestigated the effects of pressure on T_c in Hg-HTSCs using high-pressure-synthesized dense polycrystalline samples and nearly hydrostatic pressures. Recently, we briefly reported that T_c above 150 K could be achieved with zero resistivity in pressurized Hg1223 (ref. 10). In the present work, we study the pressure dependence of T_c in both Hg1212 and Hg1223 over a wide range of doping level; for Hg1212 a large and critical doping dependence of the pressure effect on T_c is revealed, while for Hg1223 the T_c with zero resistivity increases monotonously with pressure and reaches a maximal value of 153 K at 22 GPa.

Results

Doping dependence of resistivity at ambient pressure.

Figure 1a,b show the crystal structures of Hg1212 and Hg1223. These structures offer advantages for investigation of pressure effects. One is the flatness of conductive CuO₂ layer¹¹, which would be an important factor for the observed highest T_c in HTSCs. This is attributed to coordination of the CuO₂ layer with an elongated Cu–O pyramid, which has a long distance (2.7208(3) Å) between the apical-O (O_a) and Cu owing to a short covalent bond (1.972(3) Å) between Hg and O_a (ref. 11). Another advantage is that the so-called charge-reservoir block-layer (HgO_δ) is located away from the CuO₂ layer, therefore the extra oxygen least affect local distortion or least cause random potential in CuO₂ layers. Comparison of high pressure effects in Hg1212 and Hg1223 are also interesting, because Hg1212 is composed of only the equivalent two outer CuO₂ layers with an apex-elongated pyramid, while Hg1223 has extra one inner layer of CuO₂ square plane sandwiched by the two outer CuO₂ layers.

The temperature (T) dependences of electrical resistivity (ρ) in Hg1212 and Hg1223 at AP are shown in Fig. 1c,d. The doping variations in ρ - T curves exhibit common features of in-plane resistivity of HTSC cuprates¹². The insets show the dc-susceptibility and resistivity of nearly optimally doped samples and confirm that the diamagnetic (Meissner effect) signal starts at the temperature of zero resistivity. This defines the temperature of the superconducting transition, and in the following we adopt such a zero-resistivity temperature as T_c .

Hole doping level of each sample was estimated from the experimentally established relationship between hole doping and T_c reported in ref. 13, as shown in Fig. 1e,f. Values of T_c were determined from the temperature at which the diamagnetic signal begins to appear. We set $\Delta p = p - p_{\max}$, where p_{\max} gives the maximum T_c at AP in the system; by definition, $\Delta p < 0$ for the underdoped samples and $\Delta p > 0$ for the overdoped samples. Note that the variation in hole concentration of Hg1212 is wider than that of Hg1223. It was difficult to obtain an enough overdoped sample for Hg1223, even after it was annealed under high-pressure oxygen.

Doping dependence of resistivity at high pressures. The ρ - T curves of Hg1212 and Hg1223 up to 11–13 GPa are shown in Fig. 2. To facilitate visualization, the resistivities are normalized by the respective values at 270 K, while the absolute values of resistivity reduce by 30–70% from AP to 11–13 GPa. In both Hg1212 and Hg1223, the ρ - T curve in the underdoped ($\Delta p < 0$) region gradually changes from an upward convex to a straight line, though the degree of the change depends on the initial Δp values. The superconducting transition itself remains sharp, even at high pressure over 10 GPa. In the positive Δp (overdoped) region for Hg1212, however, the ρ - T curve is convex downward typical of a normal metal, while the superconducting transition becomes broader with increasing pressure. The origin of the broadened transition under pressures in the overdoped region for Hg1212 is not clear, but such a conspicuous broadening in the resistive transition is also seen for the underdoped region under higher pressures (for example, >15 GPa) where T_c turns to decrease with further application of pressure. (We come back to this problem with speculative discussion.) Note that the T_c 's for the Hg1212 samples with $\Delta p = 0.045$ (d) and $\Delta p = 0.113$ (e) show non-monotonous pressure dependence, namely at first increase and then decrease with increasing pressure. The reason for the rapid increase in T_c at relatively low pressure may be ascribed to a pressure-induced structural change, such that the apical oxygen rapidly approaches the CuO₂ layer¹⁴. Details pressure dependences of T_c and dT_c/dp in Hg1212 and Hg1223 are shown in the Supplementary Fig. 1.

Figure 3 shows the Δp dependence of T_c in Hg1212 and Hg1223. Figure 3a exemplifies the variation of T_c between at AP and 12 GPa in Hg1212. The values of T_c in the samples with negative Δp are increased by more than 30 K with application of pressure up to 12 GPa; notably in the most underdoped ($\Delta p = -0.113$) sample the T_c is increased as much as by 41 K. In contrast, the samples with positive Δp show the pressure-induced reduction of T_c . Such a clear reduction of T_c with pressure has rarely been reported in HTSC cuprates except for overdoped Tl₂Ba₂CuO_{6+δ} (Tl2201) (ref. 15). In Hg1223, on the other hand, T_c is simply increased by about 20 K from AP up to 12 GPa in each sample shown in Fig. 3b irrespective of positive and negative value of Δp , while the pressure effect on T_c appears smaller as compared with those for Hg1212 (cf. Supplementary Fig. 1).

Figure 3c,d shows T_c values as a function of Δp at various pressures (at interval of 2 GPa) for Hg1212 and Hg1223,

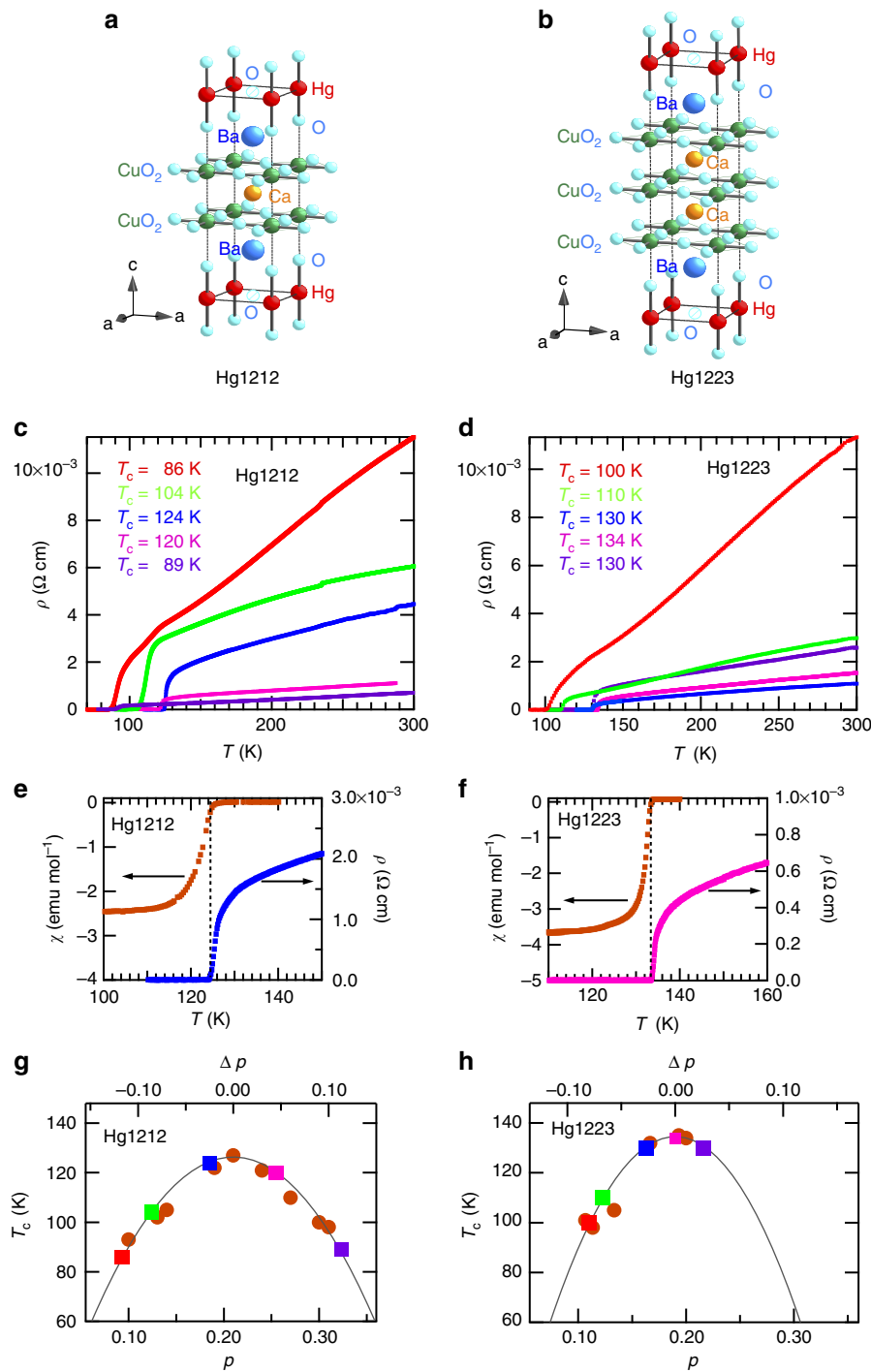


Figure 1 | Characterization of Hg1212 and Hg1223. (a,b) Crystal structure models of Hg1212 (a) and Hg1223 (b). Red, blue, yellow, green and light blue spheres correspond to Hg, Ba, Ca, Cu and O, respectively. Hashed circle indicates partially occupied oxygen. (c,d) Temperature dependence of resistivity (ρ - T) of Hg1212 (c) and Hg1223 (d) with various T_c . Colour of the curve corresponds to the text colour of T_c . (e,f) Correlation between ρ - T and temperature dependence of dc-susceptibility (χ - T) curves exemplified for Hg1212 ($T_c = 124$ K) and Hg1223 ($T_c = 134$ K). (g,h) Estimation of hole concentration (p) for Hg1212 (g) and Hg1223 (h) from a fitting curve (line) using the data in ref. 13 (solid circle). Squared symbols are data of present study. Colour of the symbol corresponds to the colour of the resistivity in panels of (c,d). Δp stands for the value measured from the optimal doping value at ambient pressure; namely, $\Delta p < 0$ for underdoped and $\Delta p > 0$ for overdoped samples.

respectively. The parabolic solid lines represent the fitting curves connecting the constant-pressure T_c s. This parabolic fitting to the Δp versus T_c dome appears to fail to cover the overdoped region, for example, $\Delta p = 0.113$ for Hg1212, yet can work well for the extrapolation to determine the maximal T_c and the corresponding Δp value. From these curves, we obtain the realizable maximal T_c

and the corresponding Δp at respective pressure values, as shown in Fig. 3e,f. Those plots show a clear tendency that the maximal T_c is attained at lower Δp and higher pressures. We can also see such correlation in the T_c contour maps on the doping–pressure diagram in Fig. 3g,h. All these analyses suggest that the maximal T_c under pressures does not always occur at the optimal doping

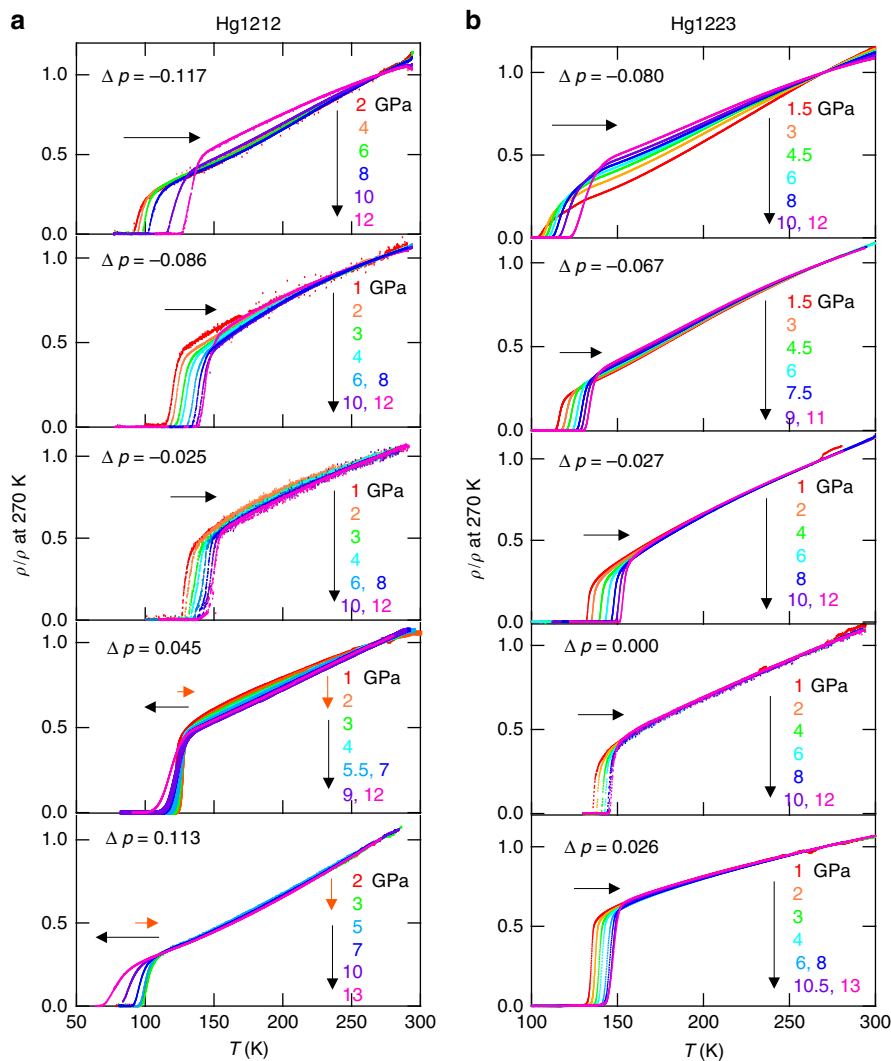


Figure 2 | Temperature dependence of electrical resistivity of Hg1212 and Hg1223 at high pressures. (a,b) Temperature dependence of electrical resistivity normalized at 270 K for Hg1212 (a) and Hg1223 (b) samples with wide doping levels indicated by Δp . Colour of the curve corresponds to the text colour of pressure.

level at AP; the optimal doping giving rise to the highest T_c does depend on the pressure value. The possible highest T_c is expected at lower doping levels and higher pressures. In practice, however, it was difficult to generate a hydrostatic pressure above 13 GPa in the present pressure load cell with an anvil size of 4 mm side.

Resistivity at high pressure over 20 GPa. To realize a higher T_c , we tried to generate higher pressures using a newly developed anvil of 3 mm side. This enabled us to achieve a nearly hydrostatic pressure up to 22 GPa, which, to the best of our knowledge, would be the highest pressure attained with a cubic-anvil press for resistivity measurements. The detailed procedure and specification for the higher pressure measurement will be reported elsewhere. In this work, we applied pressures of up to 19–22 GPa on four samples; Hg1212 with $\Delta p = -0.062$, and Hg1223 with $\Delta p = -0.030$, -0.052 and -0.095 to explore the possible highest T_c s (zero resistance) under realistic hydrostatic pressures. The hole doping levels of these samples should be nearly optimal to enhance T_c at around 20 GPa as expected from the results shown in Fig. 3c–h. Effects of pressure on T_c for the Hg1212 and the Hg1223 samples are shown in Fig. 4a,b together

with $T_{c\text{mid}}$ (peak temperature in $d\rho/dP$ curve) and $T_{c\text{onset}}$ (temperature for resistivity to start declining towards zero resistivity). Temperature dependences of resistivity are shown in Fig. 4c,d. Those for the other samples of Hg1223 are shown in Supplementary Figs 2 and 3.

For Hg1212, T_c increases up to 12 GPa with the maximum T_c of 140 K; above 12 GPa, T_c (as defined by zero resistance) decreases although the onset temperature for the resistivity reduction, $T_{c\text{onset}}$, continues to rise. The ρ – T curve is slightly convex upward and the transition width suddenly becomes broad above 12 GPa, as observed in the overdoped samples of Hg1212 (see Fig. 2d,e). In Hg1223, T_c increases up to 22 GPa with the maximum T_c of 153 K. Above 19 GPa, T_c appears to saturate, although $T_{c\text{mid}}$ and $T_{c\text{onset}}$ continue to increase, as observed in the former study¹⁰. Thus, there still remains the possibility of further increasing T_c by applying higher pressure to samples with even lower Δp .

Discussion

In the following, we discuss the possible origins of the observed conspicuous pressure effects on T_c . At first, we should note the

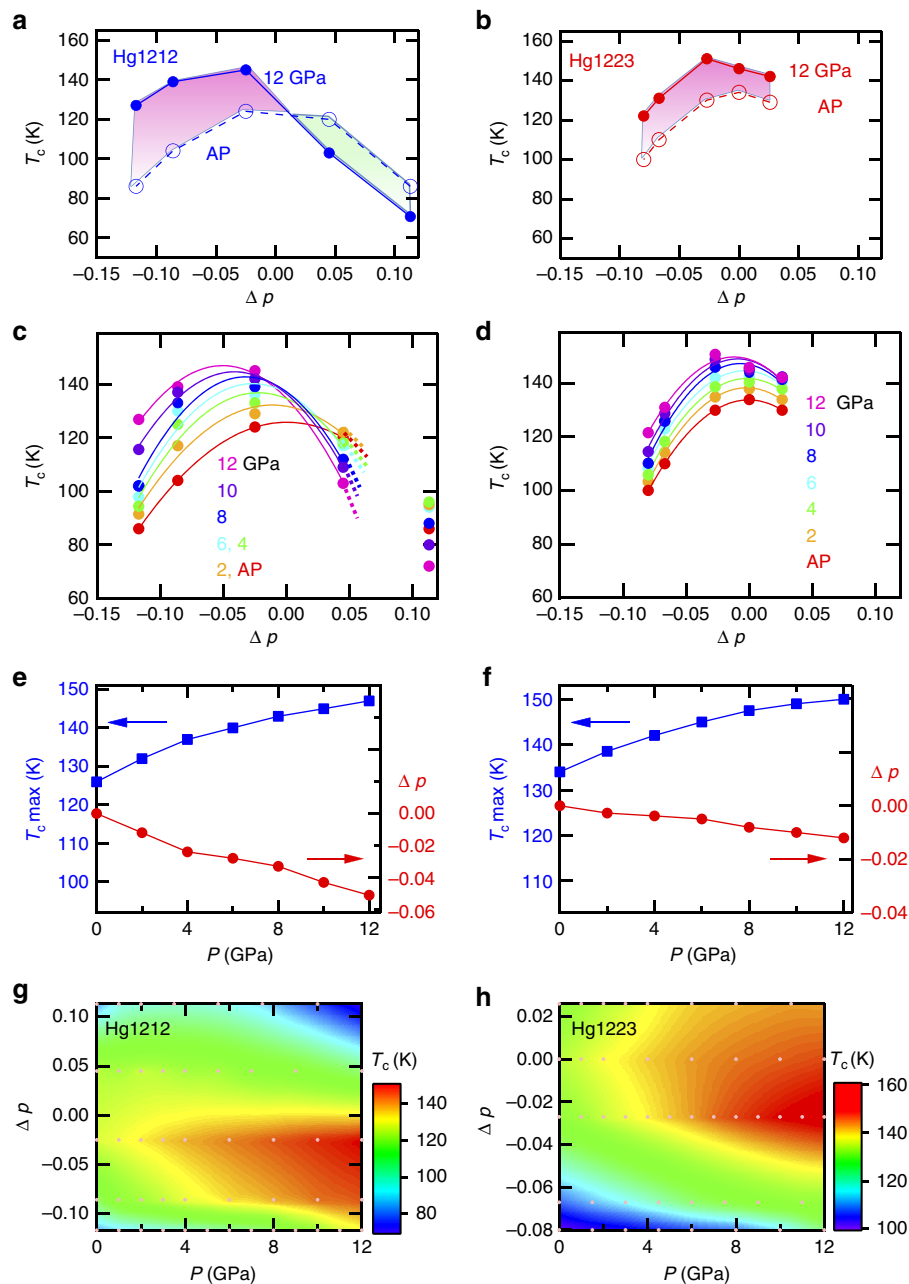


Figure 3 | Effects of pressure on T_c of Hg1212 and 1223. (a,b) Hole doping level (Δp) dependence of T_c in Hg1212 (a) and Hg1223 (b) at ambient pressure (filled circle and solid line) and 12 GPa (open circle and dashed line). Areas filled with pink and green show T_c -increased and—decreased, respectively, with pressure. (c,d) Measured and interpolated values of T_c as a function of Δp for Hg1212 (c) and Hg1223 (d) at high pressures. The parabolic solid lines show the fitting for the constant-pressure T_c versus Δp curves. Colour of the line and circle corresponds to the text colour of the pressure. (e,f) Pressure (P) dependence of T_c maximum (blue square) and Δp (red circle) that provides T_c maximum for Hg1212 (e) and Hg1223 (f). These values are estimated by the fitting curves of panel (c,d). (g,h) T_c contour maps on pressure doping level (P - Δp) diagram in Hg1212 (g) and Hg1223 (h). A colour bar shows T_c value in Kelvin. The dots in pale pink correspond to the measured data points.

highly non-monotonous pressure dependence of T_c in heavily underdoped samples (for example, Hg1212 with $\Delta p = -0.11$ and Hg1223 with $\Delta p = -0.08$) as shown in Fig. 3g,h and more clearly seen in Supplementary Fig. 3; at the first stage of applying pressure, T_c does not rise so much, but above 7–8 GPa suddenly increases with the high rate, and then the rate becomes moderate again. This newly found behaviour in T_c - P curve for the underdoped region might trace the T_c plateau and jump in the T_c - p curve, indicative of the charge order or stripe order that is characteristic of the low-doped CuO_2 sheet with the reduced T_c (ref. 16); such a charge order instability may be

removed by pressure above some critical value, for example, 7–8 GPa in the present case.

Next, we focus on the difference between the effects for Hg1212 and Hg1223 as exemplified in Fig. 3a,b. The Hg1212 shows clear increase and decrease in T_c with application of high pressure in the underdoped and overdoped regime, respectively, while the Hg1223 always shows the increase. One possible reason for this different doping dependence is the fact that only the narrower doping range can be prepared (or the enough overdoped state is difficult to form) for Hg1223 as compared with Hg1212. Another more essential reason is the presence of nonequivalent, that is,

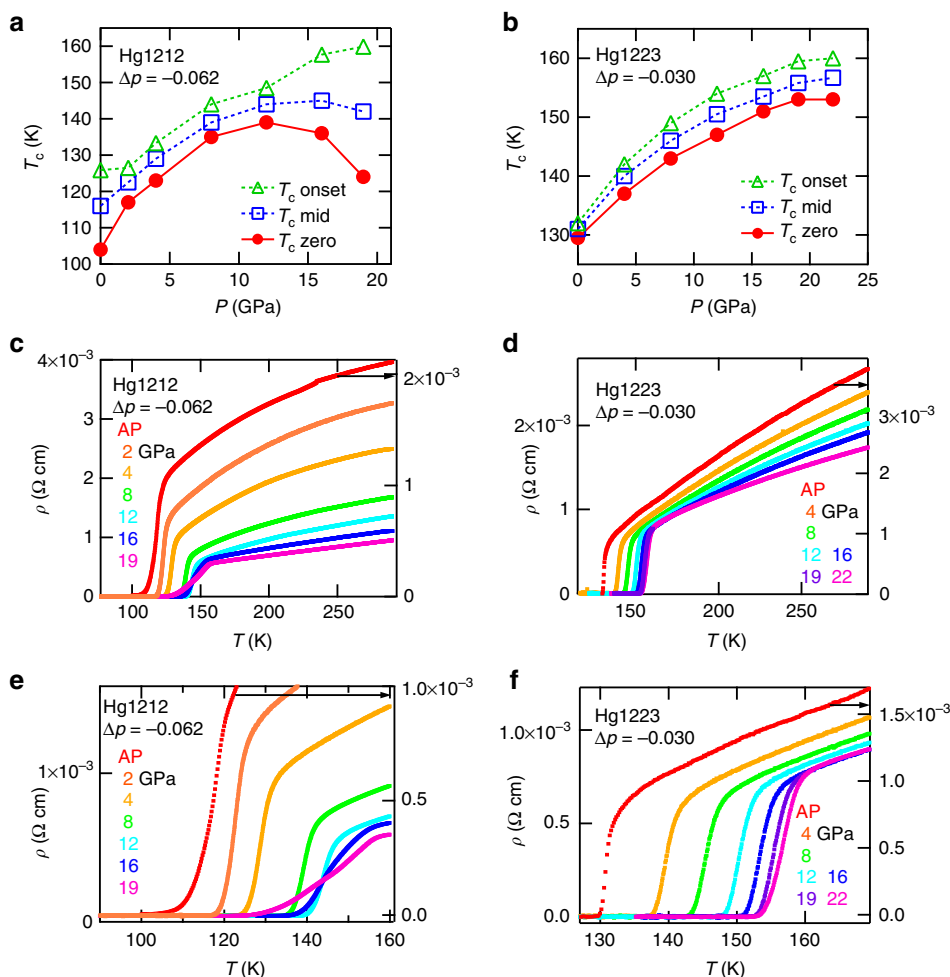


Figure 4 | Effects of higher pressure on superconductivity in Hg1212 and Hg1223. (a,b) Pressure (P) dependence of $T_{c\text{ zero}}$ (zero resistivity), $T_{c\text{ mid}}$ (a peak position of $d\rho/dT$ in superconducting transition), and $T_{c\text{ onset}}$ (the resistivity to start to decrease toward zero, as defined by a rising edge in $d\rho/dT$) for Hg1212 (a) and Hg1223 (b). (c,d) Temperature dependence of electrical resistivity (ρ - T) for Hg1212 (c) and Hg1223 (d) Colour of curve corresponds to the text colour of pressure. (e,f) Zoom-up figures of (c-f).

inner and outer, CuO_2 layers involved in Hg1223. A former NMR study suggests that the copper valence of the inner layer of $\text{HgBa}_2\text{Ca}_4\text{Cu}_5\text{O}_{12+\delta}$ (Hg1245) and $\text{TlBa}_2\text{Ca}_3\text{Cu}_4\text{O}_{10+\delta}$ (Tl1234) are lower than those of the outer layer¹⁷. Redistribution of hole carriers is likely induced among the inner and outer CuO_2 sheets in Hg1223 by applying pressure, which makes the mechanism of pressure-induced T_c -change in Hg1223 more elusive than in Hg1212 where the hole-dopable unit is restricted to the crystallographically equivalent CuO_2 sheets with the Cu-O pyramidal coordination. Thus the steeper increase (decrease) of T_c with pressure in an underdoped (overdoped) regime should be viewed as the intrinsic feature of the CuO_2 sheets.

From the analyses shown in Fig. 3, in particular for Hg1212, we obtained the result that T_c maximum can be realized when starting from an underdoped sample rather than starting from an optimally doped sample. The initial doping level that provides the maximum T_c depends on the pressure value, as indicated in Fig. 3e,f. The steep increase and then decrease of T_c with pressure as seen in the underdoped ($\Delta p = -0.062$) Hg1212 (Fig. 4a) indicates the empirical tendency that application of hydrostatic pressure effectively drives the system toward the overdoping regime; in this particular compound, for example, T_c (zero resistance) tends to decrease as the pressure exceeds 12 GPa, as if the compound were placed in the overdoped state (see Fig. 4a). Furthermore, being characteristic of the overdoped Hg1212

samples (Fig. 2e), the superconducting resistive transition becomes broadened in temperature, as manifested by a large discrepancy between $T_{c\text{ onset}}$ and T_c (zero resistance) in the $P = 16$ and 19 GPa data of Fig. 4a. In particular, the high pressure (19 GPa) value of $T_{c\text{ onset}}$ for Hg1212 reaches 160 K as high as in the case of Hg1223 (Fig. 4b). This is the feature commonly observed in previous high-pressure studies^{8,9} on this highest T_c superconductor family. The origin of this broadening of the resistive transition with higher $T_{c\text{ onset}}$ but lower T_c (zero resistance) in the effectively pressure-induced overdoping regime is still not clear; it is hardly ascribable to the pressure inhomogeneity at least in the present experiment, since the superconducting transition under around 20 GPa for Hg1223 (see Fig. 4d) remains as sharp as at lower pressures. We speculate that the pressure-driven overdoped state may show the tendency of some intrinsic electronic phase separation into the higher T_c (> 160 K) filaments or embryos and the lower T_c (< 160 K) state above 20 GPa; however, this issue remains as an important subject of future study.

Methods

Sample preparation at high pressure. The polycrystalline samples of Hg1212 and Hg1223 were synthesized with a cubic-anvil-type high-pressure apparatus (180 ton press, TRY Eng. Co.). Mixtures of HgO, BaO_2 , CaO, and CuO/Cu, or mixtures of HgO and the precursor (prepared from BaCO_3 , CaO and CuO at

950 °C in a flowing high-purity oxygen gas) were placed into a cylindrical gold capsule and sintered for 10–30 min at 805–850 °C under a pressure of 2 GPa. To control the hole doping level, we have optimized the starting material, sintering condition, and annealing condition for each sample. Details are described in Supplementary Table 1.

Sample characterization. The optimized nominal compositions to obtain single-phase materials were $\text{Hg}_{0.85}\text{Ba}_2\text{CaCu}_{2.15}\text{O}_{6+\delta}$ for Hg1212 and $\text{Hg}_{0.75}\text{Ba}_2\text{Ca}_2\text{Cu}_{3.25}\text{O}_{8+\delta}$ for Hg1223. The analysed compositions determined by a scanning electron microscope (JSM-6701 F, JEOL) equipped with energy dispersive X-ray analyzer (XFlash detector 5030, Bruker AXS) were Hg:Ba:Ca:Cu = 0.77:1.99:0.99:2.25 and 0.81:1.96:2.17:3.07, respectively. The powder X-ray diffraction patterns (RINT, Rigaku) confirmed the nearly single phase of Hg1212 and Hg1223. The scanning electron microscope images indicate that they are much denser than the samples prepared with the conventional silica-tube encapsulation method. The bulk superconductivity at ambient pressure was confirmed by dc-susceptibility measured with the field cooling procedure at 20 Oe (MPMS, Quantum Design) as well as by electrical resistivity (PPMS, Quantum Design).

Resistivity measurement at high pressure. The electrical resistivity at high pressure was measured using a cubic-anvil-type high-pressure apparatus with low-temperature cryostat (200 ton press, Rockgate Co.). The samples with the four gold wires were placed in Teflon capsule with grease (Apiezon N) as a pressure-transmitting medium, and put in the gasket of MgO. To produce higher pressure, we use anvil tops with the sintered diamond. The anvils with the size of $4 \times 4 \text{ mm}^2$ (sample size: $1.2 \times 0.6 \times 0.4 \text{ mm}^3$) and of $3 \times 3 \text{ mm}^2$ (sample size: $0.8 \times 0.4 \times 0.3 \text{ mm}^3$) were used for the experiments up to 13 and 22 GPa, respectively. The sample temperature was determined with the Cernox resistance thermosensor on one of the anvil top.

References

- Drozhdov, A. P., Erements, M. I., Trojan, I. A., Ksenofontov, V. & Shylin, S. I. Conventional superconductivity at 203 kelvin at high pressures in the sulfur hydride system. *Nature* **525**, 73–76 (2015).
- Deemyad, S. *et al.* Dependence of the superconducting transition temperature of single and polycrystalline MgB_2 on hydrostatic pressure. *Physica C Supercond.* **385**, 105–116 (2003).
- Garbarino, G. *et al.* High-temperature superconductivity (T_c onset at 34 K) in the high-pressure orthorhombic phase of FeSe. *Europhys. Lett.* **86**, 27001 (2009).
- Takahashi, H. & Tomita, T. High pressure effect for high- T_c superconductors. *J. Cyro. Soc. Jpn.* **46**, 203–211 (2011).
- Putlin, S. N., Antipov, E. V., Chmaissem, O. & Marezio, M. Superconductivity at 94 K in $\text{HgBa}_2\text{CuO}_{4+\delta}$. *Nature* **362**, 226–228 (1993).
- Shilling, A., Cantoni, M., Guo, J. D. & Ott, H. R. Superconductivity above 130 K in the Hg–Ba–Ca–Cu–O system. *Nature* **363**, 56–58 (1993).
- Iyo, A. *et al.* Variation of T_c in multilayered cuprates of $\text{HgBa}_2\text{Ca}_{n-1}\text{Cu}_n\text{O}_y$. *Physica C* **460–462**, 436–437 (2007).
- Gao, L. *et al.* Superconductivity up to 164 K in $\text{HgBa}_2\text{Ca}_{m-1}\text{Cu}_m\text{O}_{2m+2+\delta}$ ($m=1, 2$, and 3) under quasihydrostatic pressures. *Phys. Rev. B* **50**, 4260–4263 (1994).
- Monteverde, M. *et al.* High-pressure effects in fluorinated $\text{HgBa}_2\text{Ca}_2\text{Cu}_3\text{O}_{8+\delta}$. *Europhys. Lett.* **72**, 458–464 (2005).
- Takeshita, N., Yamamoto, A., Iyo, A. & Eisaki, H. Zero resistivity above 150 K in $\text{HgBa}_2\text{Ca}_2\text{Cu}_3\text{O}_{8+\delta}$ at high pressure. *J. Phys. Soc. Jpn.* **82**, 023711 (2013).
- Wagner, J. L., Hunter, B. A., Hinks, D. G. & Jorgensen, J. D. Structure and superconductivity of $\text{HgBa}_2\text{Ca}_2\text{Cu}_3\text{O}_{8+\delta}$. *Phys. Rev. B* **51**, 15407–15414 (1995).
- Ando, Y., Komiya, S., Segawa, K., Ono, S. & Kurita, Y. Electronic phase diagram of high- T_c cuprate superconductors from a mapping of the in-plane resistivity curvature. *Phys. Rev. Lett.* **93**, 267001 (2004).
- Fukuoka, A. *et al.* Dependence of T_c and transport properties on the Cu valence in $\text{HgBa}_2\text{Ca}_{n-1}\text{Cu}_n\text{O}_{2(n+1)+\delta}$ ($n=1, 2, 3$) superconductors. *Phys. Rev. B* **55**, 6612–6620 (1997).
- Gatt, R. *et al.* Pressure effect in the Hg-based superconductors: A structural study. *Phys. Rev. B* **57**, 13922–13928 (1998).
- Klehe, A.-K. *et al.* Pressure-induced oxygen ordering phenomena in high- T_c superconductors. *Physica C Supercond.* **257**, 105–116 (1996).
- Comin, R. *et al.* Symmetry of charge order in cuprates. *Nat. Mater.* **14**, 796–800 (2015).
- Mukuda, H. *et al.* Uniform mixing of high- T_c superconductivity and antiferromagnetism on a single CuO_2 plane of a Hg-based five-layered cuprate. *Phys. Rev. Lett.* **96**, 087001 (2006).

Acknowledgements

The authors thank Drs H. Eisaki, A. Iyo, M. Mito, Y. Nohara and R. Arita for fruitful discussions. This work was in part supported by Grants-in-Aid for Scientific Research (No. 23340110, No. 26289091) from the MEXT, Japan.

Author contributions

Y.T. conceived the project. The samples were synthesized by A.Y., and the resistivity measurements at high pressures were performed by N.T., A.Y. and C.T. The results were discussed by A.Y., N.T. and Y.T. A.Y. and Y.T. wrote the manuscript.

Additional information

Supplementary Information accompanies this paper at <http://www.nature.com/naturecommunications>

Competing financial interests: The authors declare no competing financial interests.

Reprints and permission information is available online at <http://npg.nature.com/reprintsandpermissions/>

How to cite this article: Yamamoto, A. *et al.* High-pressure effects revisited for the cuprate superconductor family with highest critical temperature. *Nat. Commun.* 6:8990 doi: 10.1038/ncomms9990 (2015).



This work is licensed under a Creative Commons Attribution 4.0 International License. The images or other third party material in this article are included in the article's Creative Commons license, unless indicated otherwise in the credit line; if the material is not included under the Creative Commons license, users will need to obtain permission from the license holder to reproduce the material. To view a copy of this license, visit <http://creativecommons.org/licenses/by/4.0/>